Development of a methodology for the application of synthetic DNA in stream tracer injection experiments

Jan Willem Foppen,[1] Judith Seopa,[1] Noel Bakobie,[1] and Thom Bogaard[1,2]

Received 5 September 2012; revised 18 July 2013; accepted 18 July 2013.

[1] Stream tracer injection experiments are useful for characterizing hydrological and biogeochemical processes in streams. We used nonconservative synthetic DNA and conservative NaCl in six instantaneous tracer injection experiments in streams in the Benelux. The main aim was to compare the performance of injected synthetic DNA tracer "T23" with NaCl. In all experiments, the shapes of the T23 and NaCl breakthrough curves (BTCs) were similar. Recovered T23 mass ranged from 2.9 to 52.6%, while recovered NaCl tracer mass ranged from 66.7% to complete mass recovery. In batch experiments, T23 decay was not detected. However, in those batches, we observed an unexplained initial T23 mass loss of 40–97%. In batches with sediment, T23 attachment rate coefficients ranged from close to zero to 0.2 hr^{-1}. Advective and dispersive transport parameters of both NaCl and T23 fitted with STAMMT-L were similar. However, compared to T23, fitted storage zone areas of NaCl were 2–5 times larger, while storage zone exchange coefficients were two times larger. Fitted mass dilution factors of T23 ranged from 1.6 to 34.8. Together, these results pointed toward the disappearance of a part of the T23 mass due to both initial losses and attachment or sorption of T23 mass in those storage zone(s), while decay was not important. Our research demonstrated that artificial DNA can be a valuable tool to determine advective and dispersive transport in brooks, but not to assess solute mass exchange processes related to surface transient storage or hyporheic exchange.

Citation: Foppen, J. W., J. Seopa, N. Bakobie, and T. Bogaard (2013), Development of a methodology for the application of synthetic DNA in stream tracer injection experiments, *Water Resour. Res.*, *49*, doi:10.1002/wrcr.20438

1. Introduction

[2] Stream tracer injection experiments are useful for characterizing hydrological and biogeochemical processes in streams, especially in transient storage zones within streams. In such tracer injection experiments, usually one or two artificial solute tracers are injected into a stream, and then, by fitting a model to the tracer breakthrough curves (BTCs), the size and extent of the storage zone and the exchange rate can be determined [*Runkel*, 1998; *Choi and Harvey*, 2000]. *Harvey et al*. [1996] and *Wagner and Harvey* [1997] discussed that the shoulder and tail of a solute BTC contain most information for transient storage modeling (TSM). However, artificial tracer injection experiments lack spatial coverage, thereby limiting accurate quantification of spatially heterogeneous exchange dynamics [*Ward et al*., 2010]. Only recently stream solute transport science has begun to address the importance of multiple scales of storage, e.g., surface versus hyporheic transient storage [*Gooseff et al*., 2003; *Ward et al*., 2010], and to develop field methods to identify multiple scale transient storage in river systems [*Briggs et al*., 2009; *Gooseff et al*., 2011].

[3] A multitracer approach can overcome the problem of lack of spatial coverage. According to *Gourcy and Brenot* [2011], new environmental tracers such as Sr, B, and SO4 isotopes, as well as chlorofluorocarbons (CFCs) and SF6 [e.g., *Vengosh et al*., 2002; *Négrel and Pauwels*, 2004; *Négrel and Petelet-Giraud*, 2005; *Gooddy et al*., 2006] have been successfully applied in multitracer approaches, and also for an improved understanding of the interaction between groundwater and surface water [*Oxtobee and Novakowski*, 2002; *Lamontagne et al*., 2005; *Darling et al*., 2010]. In addition, *Haggerty et al*. [2009] used the reactive tracer resazurin to assess hyporheic exchange within river systems. The use of a truly "multi"tracer approach with artificial tracers is not widely documented. In the framework of TSM, artificial tracers are rarely used in combination with each other, either because their use in surface waters is prohibited (e.g., the use of fluorescein and rhodamine is prohibited in parts of Europe) or because methods of detection are laborious and/or too different.

[4] In the late 1990s, special tracing techniques involving synthetic DNA (deoxyribonucleic acid) molecules were developed [*Alestrom*, 1995], and successfully applied in various field experiments related to groundwater flow in

Additional supporting information may be found in the online version of this article.

[1]UNESCO-IHE Institute for Water Education, Delft, Netherlands.
[2]Water Resources Section, Delft University of Technology, Delft, Netherlands.

Corresponding author: J. W. Foppen; UNESCO-IHE Institute for Water Education, P.O. Box 3015, 2601 DA Delft, Netherlands. (j.foppen@unesco-ihe.org)

©2013. American Geophysical Union. All Rights Reserved.
0043-1397/13/10.1002/wrcr.20438

Table 1. Criteria Used for the Design of DNA Tracers, Primers, and Probes Used in This Research

Parameter	Tracer Sequence	Primer(s)	Probe
Length	80 Nucleotides	20 Nucleotides	24 Nucleotides
GC-content	40–60%	40–60%	40–60%
Annealing temp		55–60°C	55–60 + 8–10°C
3′-end		Not GGG, not T	
5′-end			Not G
Complementarities		None	None
BLAST search (nr/nt)	None	No similarity found	No similarity found
BLAST with primers	No similarity found	No template found	
BLAST with primer(s) and probe			No template found

aquifers [*Sabir et al*., 1999, 2000]. With such new tracer compounds, it became possible to perform multitracer experiments with a theoretically unlimited number of tracers. By showing the presence or absence in water samples, Sabir and workers determined in a qualitative way flow patterns and velocities in various complex-fractured hard rock aquifers. Finally, *Foppen et al*. [2011] showed that synthetic DNA tracers could be used quantitatively as tracer in natural streams. However, a rigorous assessment of the applicability of this novel tracer was not yet carried out.

[5] In this research, we look in detail at the behavior of one synthetic DNA tracer in stream tracer injection experiments and we compare its performance with NaCl, a conservative tracer. Thereto, we present a quantitative analysis of the transient DNA mass balance of six tracer injection experiments. We assess the potential of artificial DNA, the limitations and we discuss future applications. In addition, we describe and discuss our methodology or protocol for using synthetic DNA in stream tracer injection experiments. In order to enhance the readability of our work, the hydrological aspects are discussed in this "main" document, while the molecular microbiological aspects and considerations are discussed in supporting information.

2. Materials and Methods

2.1. Preparation of DNA Tracers

[6] We used single stranded DNA tracers with a length of 80 nucleotides. Nucleotide positions 1–20 were reserved for the forward primer, and position 61–80 for the reverse primer; positions 30–54 were reserved for the so-called Taqman probe. We chose to use Taqman probes because of their improved selectivity compared to the fluorescent dye SYBR-Green, which we used in our earlier work [*Foppen et al*., 2011]. The probe was labeled with a 6-carboxyfluorescein (FAM) fluorophore on one side and a Black Hole Quencher (BHQ) on the other side. DNA tracers were randomly generated, and the entire sequence, the primers, and the probe were subsequently checked for a number of boundary conditions (Table 1) in order to reduce problems during the quantitative polymerase chain reaction (qPCR). Furthermore, the randomly generated DNA sequences were unique, which was determined with an online BLAST search at the National Center for Biotechnology Information (www.ncbi.nlm.nih.gov). For this research, we designed two DNA tracers: T22 and T23 (Table 2). DNA tracers, primers, and probes were manufactured by Biolegio (Nijmegen, Netherlands), and DNA tracer quantities obtained in this way ranged from 2 to 6×10^{16} particles.

2.2. Tracer Injection Experiments

2.2.1. Description of Experimental Areas

[7] We selected two brooks in Luxembourg, the Maisbich and the Heuwelerbach, and two brooks on the border of Netherlands and Belgium, the Gelsloopken (Gloop) and the Biezenloop (Bloop). We carried out six instantaneous tracer injection experiments with DNA tracer and NaCl (see Tables 3 and 4).

[8] The Maisbich catchment [*Westhoff et al*., 2011] has an area of 0.342 km^2, the elevation ranges from 296 to 494 m.a.s.l., and it consists of schist lithology. The slopes of the catchment have been eroded into colluvial deposits, which are in part overlain by thin alluvial deposits of the Maisbich. The upper area of the catchment is generally pasture, while the lower part of the area consists of deciduous forest. In the Maisbich, we carried out two experiments in February 2012: one in the downstream part of the catchment (Mais-down) with two measuring points at 100 and 400 m from the point of injection and one in the upstream part of the catchment (Mais-up), where between point of injection and measurement the stream partly disappeared and a few meter downstream reappeared into the alluvial/

Table 2. Nucleotide Sequences of DNA Tracers T22 and T23 and the Compositions of Their Primers and Probes

Tracer Part Description	Nucleotide Sequence
Marker T22	3′-[F-Primer]-ACAGGTAGG-Probe-AGTATCA-[R-Primer]-5′
F primer	3′-GCGCTCTTGTGTACTATGAA-5′
R-primer	3′-TCGACCTTCATTCCTCGCTA-5′
Probe	3′-AGAGTTCGAATGTGATGGCCTAAA-5′
Marker T23	3′-[F-Primer]-AGCTATAGG-Probe-GCGAAGC-[R-Primer]-5′
F-primer	3′-ATGACGACGGCCAGTAATAT-5′
R-primer	3′-ATGCGCCTCGAGCTTCTAAA-5′
Probe	3′-TTGACTCAGAGCTTACCCTCATAA-5′

Table 3. DNA T23 Mass Injected and Mass Recovered of All Tracer Injection Experiments

Experiment	Distance (m)	Q (l/s)	DNA Mass Injected (Number of Part.)	DNA Mass Recovered (Number of Part.)	DNA Mass Recovered (% of Mass Injected)
Mais-down	100		$(1.32 \pm 0.55)\cdot10^{15}$	$(4.31 \pm 1.81)\cdot10^{14}$	32.7 ± 13.7
	400	34		$(2.12 \pm 0.89)\cdot10^{14}$	16.1 ± 6.7
Mais-up	150	11	$(5.02 \pm 2.11)\cdot10^{14}$	$(3.43 \pm 1.44)\cdot10^{13}$	6.8 ± 2.9
Heuwelerbach	300		$(8.05 \pm 3.38)\cdot10^{14}$	$(4.86 \pm 2.04)\ 10^{13}$	6.0 ± 2.5
	650	15		$(2.33 \pm 0.98)\cdot10^{13}$	2.9 ± 1.2
Ditch	150	3	$(1.02 \pm 0.43)\ 10^{15}$	$(1.39 \pm 0.58)\cdot10^{14}$	13.6 ± 5.7
Gelsloopken	300	89	$(4.40 \pm 1.85)\ 10^{16}$	$(1.08 \pm 0.45)\cdot10^{16}$	24.5 ± 10.3
Biezenloop	300		$(1.00 \pm 0.42)\ 10^{16}$	$(4.64 \pm 1.95)\cdot10^{15}$	46.4 ± 19.5
	550	20		$(5.26 \pm 2.21)\cdot10^{15}$	52.6 ± 22.1

colluvial deposits. The discharge of Mais up was 11 l/s and of Mais down 34 l/s.

[9] The Heuwelerbach catchment [*Gerrits*, 2010] covers an area of 2.7 km^2, with an elevation of 280–400 m.a.s.l., and it consists of sandstone and marls. The main land use is forest on the plateau and the slopes, whereas grasslands are found in the riparian zone and at the foot slopes [*Juilleret et al*., 2012]. The Heuwelerbach is fed by a number of springs occurring at the interface between the sandstones and the marls. Here, we carried out one injection experiment with measurement points at 300 and 650 m from the point of injection. The discharge was 15 l/s at the second point of measurement.

[10] The Gloop and Bloop are both headwaters of the Merkske catchment. Both subcatchments cover an area of 1–2 km^2 and are characterized by sand and clay deposits with elevations ranging between 15 and 20 m.a.s.l. Land use of the Gloop is dominated by grassland and maize, while Bloop is dominated by forest and heath. In the Gloop area, in January 2012, we carried out two experiments: one in a small tributary (Ditch) with low velocity and a discharge of 3 l/s, and one injection experiment in the Gloop itself with a measurement point 300 m downstream of the injection point. The Gloop had a discharge of 89 l/s. In the Bloop, also in January 2012, we carried out one injection experiment with measurement points at 300 and 550 m downstream of the point of injection. The discharge of the Bloop was 20 l/s. All discharges were measured with the instantaneous salt method [*Leibundgut et al*., 2009] and we visually estimated that the discharge remained constant during the experiment. Prior to each experiment, a 100 mL brook water sample was taken for the field batch experiment (see below). In addition, sediment grab samples were taken, stored in a 5 L PE bucket in a coolbox, and transported to the laboratory for further use.

2.2.2. Preliminary Steps in the Development of the Protocol

[11] In supporting information ("Preliminary steps in the development of the protocol"), we describe in detail the results of our analysis on the influence of various types of containers on the concentrations of DNA tracers, the effect of filtering and filter types and also of various water sample taking techniques. Here, we summarize the final methods and materials we used for our experiments.

[12] All water samples for synthetic DNA analysis were taken with a Gilson Pipetman and a 1 mL low-adhesion polypropylene disposable gradient filtertip without surface charge to assure no binding of charged molecules like DNA, and equipped with a Self Sealing NonCollapsing (SSNC) filter tip (Bioplastics, Landgraaf, Netherlands) to avoid crosscontamination. All DNA samples were stored without filtering in 1.5 or 2 mL low-adhesion polypropylene Eppendorf vials. Back in the laboratory, the Eppendorf vials with DNA were stored at $-80^{\circ}C$. For larger volumes (e.g., field batch experiments), we used polypropylene copolymer (PPCO) bottles, known for their low DNA binding capacity [*Gaillard and Strauss*, 2000]. In the field, when handling DNA, and in order to avoid cross contamination, we used latex gloves and all materials that had been in contact with DNA tracer material were immediately disposed of in designated plastic disposal bags.

2.2.3. Tracer Injection

[13] Before carrying out the DNA injection, we first injected a dissolved mass of NaCl (Table 4) and determined the electrical conductivity (EC) with an EC-meter (WTW LF323) at the downstream measurement points. In the field,

Table 4. NaCl Mass Injected and Mass Recovered of All Tracer Injection Experiments

Experiment	Distance (m)	Q (l/s)	NaCl Mass Injected (kg)	NaCl Mass Recovered (kg)	NaCl Mass Recovered (% of Mass Injected)
Mais-down	100		2.00	1.91	95.3
	400	34		1.69	84.7
Mais-up	150	11	0.45	0.30	66.7
Heuwelerbach	300		0.75	0.73	97.2
	650	15		0.71	94.3
Ditch	150	3	0.20	0.16	82.1
Gelsloopken	300	89	2.00	1.98	98.8
Biezenloop	300		2.00	2.12	106.1
	550	20		1.98	98.8

the salt BTC was used to design the DNA injection experiment, and to determine the time of first arrival, the sampling frequency and the total duration of the DNA breakthrough at the measurement point. Later, for the analysis of tracer BTCs, the EC-values were converted into injected NaCl concentration with a NaCl calibration curve using brook water.

[14] In the laboratory, prior to each injection experiment, a vial with concentrated DNA tracer solution was prepared in 450 µl TE buffer (Sigma-Aldrich product 93283), and kept frozen until the time of application, either in a cool box or on dry ice (Luxembourg experiments). In the field, the contents of the vial were mixed with 100 mL milliQ water. Three samples of 100 µL each were taken to determine the injected DNA mass. At the point(s) of measurement, samples were taken from the brook. For the Luxembourg experiments, the vials were stored on dry ice, and within 3 days transported to the laboratory; for the Gloop and Bloop experiments, the vials were stored in a coolbox and on the same day transported to the laboratory.

2.3. Batch Experiments

[15] In the field, prior to DNA injection, a 100 mL brook water sample was taken in which we injected concentrated DNA tracer solution. After manual mixing, every 5–15 min a 100 µL sample was taken. The batch experiments were carried out parallel to the DNA injection experiment in the brook. We performed these experiments to determine a DNA decay rate or inactivation coefficient. We anticipated that DNA concentrations would reduce due to consumption by microorganisms, either in the form of ingestion or transformation, and damage due to photodecay.

[16] In order to better understand the effect of sediment on DNA tracer concentration in brook water, and to assess the potential effect of attachment or sorption, 5 g of brook sediment was oven dried (at 105°C for 2 h) and placed in a bottle together with 100 mL of brook water. The grain size distribution of the sediment ranged from fine to coarse sand. To this a vial with concentrated DNA tracer solution was added. Then, at room temperature and exposed to day light, the samples were gently shaken, and samples were collected in duplicate at 1, 2, 4, 6, and 10 h. The coarse sediment in the batch remained at the bottom of the batch container for the entire duration of the experiment.

2.4. Determining DNA Tracer Concentrations

[17] DNA concentrations were determined using qPCR (Mini-Opticon; Bio-Rad, Hercules, CA, USA). From the amplification profiles of each sample, the threshold cycle was determined using the algorithm developed by *Zhao and Fernald* [2005]. By determining the threshold cycles for samples with known DNA concentrations, a standard curve can be created from which the threshold cycle of an unknown sample can be converted into DNA concentration [e.g., *Bustin and Nolan*, 2009]. The qPCR technique is robust, extremely sensitive, and its dynamic range, defined as the ratio between the largest and smallest measurable concentration without the need to dilute or otherwise pretreat the sample, can cover 8–9 log units. Details with regard to qPCR mixes used, standard curves, standard curve efficiency, individual amplification efficiencies, inhibition of the qPCR reaction, and lowest level of detection of a positive sample are presented in supporting information.

2.5. Assessing Confidence Intervals of DNA Tracer Concentrations

[18] Carrying out a qPCR analysis requires 36 pipetting actions of volumes ranging from 4 to 500 µL for each analyzed sample (see supporting information). Depending on the accuracy and precision of the pipet and pipetting system used, this gives rise to errors in the resulting DNA concentration, and it is important to quantify these errors in order to determine realistic confidence intervals of the DNA tracer concentrations. We identified two types of errors: (1) serial dilution errors (or the propagation of error in serial dilutions) and (2) random errors due to differences in performance of the qPCR apparatus and/or due to minor variations in the preparation of the qPCR mix or in adding qPCR mix and sample to a qPCR well.

2.6. BTC Fitting with STAMMT-L

[19] In order to quantitatively evaluate the mass balances of DNA and NaCl in the stream tracer injection experiments, and to compare their performances, a one-dimensional transport model with inflow and solute storage was used to simulate tracer transport. We used STAMMT-L [*Haggerty and Reeves*, 2002]. This code applies a user specified solute residence time distribution to a general one-dimensional advection dispersion transport equation

$$\frac{\partial C}{\partial t} = -\nu\frac{\partial C}{\partial x} + D\frac{\partial^2 C}{\partial x^2} - \beta_{\text{tot}}\frac{\partial C_S}{\partial t} \tag{1}$$

[20] where C is the main channel solute concentration (M/L^3), t is time (T), ν is the mean advection velocity equivalent to Q/A (L/T) (where Q is the stream flow rate (L^3/T) and A is main channel cross-sectional area (L^2)), x is distance (L), D is dispersion coefficient (L^2/T), β_{tot} is the capacity coefficient, defined as the ratio of the mass in the immobile domain to that in the mobile domain at equilibrium, or as the ratio of storage to stream cross-sectional areas, and C_S is the storage zone solute concentration (M/L^3). Storage zone concentrations are defined as

$$\frac{\partial C_S}{\partial t} = \int_0^t \frac{\partial C(t-\tau)}{\partial t} g^*(t)dt \tag{2}$$

[21] where τ is a time lag (T). STAMMT-L can handle various expressions and distributions of diffusion rate coefficients or first-order mass-transfer coefficients. In this work, we used the single first-order mass transfer expression, $g^*(t)$, which is defined as

$$g^*(t) = \omega e^{-\omega t} \tag{3}$$

[22] where ω is a first-order mass-transfer rate coefficient (T^{-1}) between the mobile and immobile phase. The advantage of using STAMMT-L is in the possibility to optimize residual calculations by comparing natural logarithms of values. In this way, differences between measured and calculated concentrations in the tail of the solute BTC become of the same order of magnitude as those during peak

breakthrough, which is advantageous if the tail of the BTC is considered to be important.

[23] Parameter fitting was carried out for ν, α_L, β_{tot}, and ω. STAMMT-L does not produce fitted dispersion coefficients; instead the longitudinal dispersivity, α_L, is determined, which is defined as

$$\alpha_L = \frac{D}{\nu} \tag{4}$$

[24] In addition to these four parameters, a mass dilution factor was fitted. Since the governing equations of STAMMT-L do not include a direct mass loss term, within the code, a mass dilution factor is used to account for mass losses

$$m_{rec} = \frac{m_{inj}}{\varphi} \tag{5}$$

[25] where m_{rec} is the mass recovered as simulated at the end of the reach (M), m_{in} is the mass injected (M), and φ is the mass dilution factor due to losses, sorption, and so on. Furthermore, instead of evaluating ω, the first-order mass-transfer rate coefficient, we preferred to evaluate the product of β_{tot} and ω, or "$\beta\omega$," the storage zone exchange coefficient, which is a direct measure of the mass exchange between the brook and transient surface or hyporheic storage zones, present in the brook [*Gooseff et al*., 2003].

3. Results

3.1. DNA Tracer Standard Curve Analysis, Error Analysis, and Background Water Quality of the Brooks

[26] The serial dilution associated with the tracer injection experiments and with the batch experiments involved six steps in a tenfold serial dilution series, meaning that we used a 10^6 to 10^{12} times serially diluted initial concentration, and this corresponded to a confidence interval of 19.2% of the input concentration. This, together with a random error of 14% of the input concentration gave a confidence interval of ~33% of the input concentration at a 95% confidence level. The confidence intervals of DNA tracer concentrations in the injection experiments were large. However, due to the large concentration range of synthetic DNA covering 4–5 logarithmic units, these confidence intervals were still acceptable, and much smaller than the concentration ranges in the BTCs (e.g., compare error bars and y axis scale in Figures 1–5).

[27] The amplification efficiency of the DNA tracers also depended on the overall water quality of the brooks. In the Gloop and Bloop humic compounds were present, evidenced by the brownish color of the brook water. In these two streams, none of the DNA tracer material in positive standard curve material was amplified in the qPCR apparatus. In order to eliminate this inhibition, samples had to be diluted 4–10 times. For the other brooks, no inhibition occurred. Despite the differences in water quality, eventually none of the standard curves were statistically different from each other at a significance level of 5%.

[28] For T22 the individual qPCR amplifications over the entire concentration range were not constant, while for T23 the individual amplifications were constant. Furthermore, for T22 more "noise" (late amplification of negative control samples) occurred than for T23, where noise was usually absent. We concluded that, despite having used exactly the same design criteria, the performance of tracer T22 in the qPCR assay was not optimal, while the performance of T23 was satisfactory. Therefore, from now on, we will focus our attention on tracer T23.

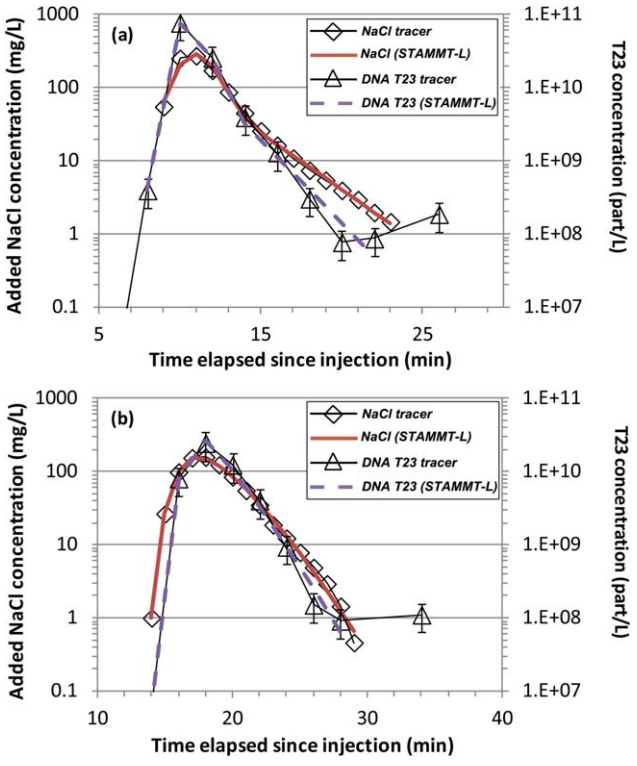

Figure 1. Mais down experiment. BTCs of salt and DNA tracer T23 (a) 100 m and (b) 400 m downstream of the point of tracer injection. Error bars indicate 95% confidence intervals.

3.2. Tracer Injection Experiments

[29] In all injection experiments, the (fast) time of the first arrival shown by the off-set on the x axis, for both NaCl and T23 in all injection experiments was similar, and

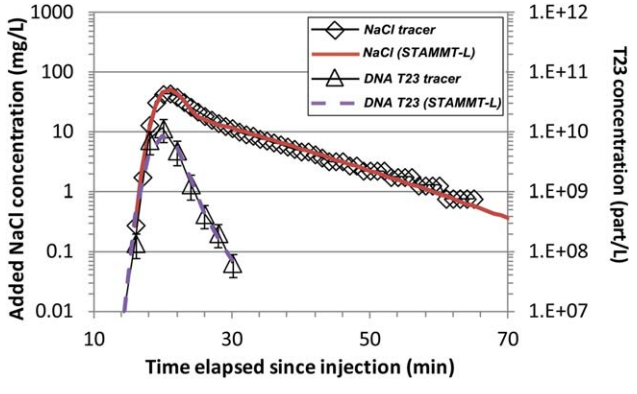

Figure 2. Mais up experiment. BTCs of salt and DNA tracer T23 150 m downstream of the point of tracer injection. Error bars indicate 95% confidence intervals.

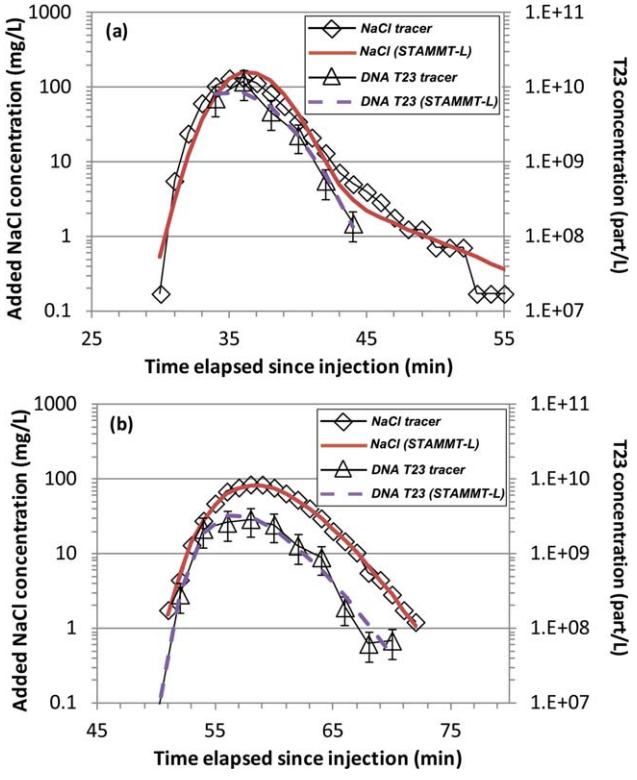

Figure 3. Heuwelerbach experiment. BTCs of salt and DNA tracer T23 (a) 300 m and (b) 650 m downstream of the point of tracer injection. Error bars indicate 95% confidence intervals.

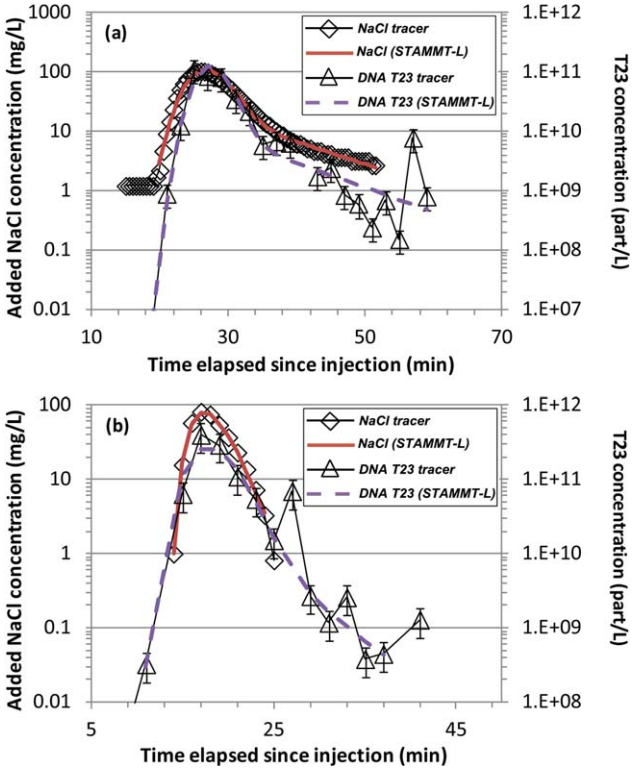

Figure 4. Gloop experiments. BTCs of salt and DNA tracer T23 (a) 150 m downstream of the injection point in the Ditch and (b) 300 m downstream of the point of tracer injection in the Gloop. Error bars indicate 95% confidence intervals.

so was the shape of the rising limb of both types of BTCs (Figures 1–5). Also, the time to peak of both the NaCl and T23 BTCs was similar. Concentrations increased to a maximum of around 200 mg/L of added NaCl and to around $(3 \pm 1.2)\cdot 10^{11}$ particles/L for T23 (e.g., Figures 5a and 5b). After the peak, concentrations decreased in a less steep, log linear fashion to background concentrations for NaCl. For T23, concentrations decreased to the lower limit of positive detection, which was 5×10^{8} part/L for the Bloop (Figure 5), 2×10^{8} part/L for the Gloop (Figure 4a), and 5×10^{7} part/L for the other brooks. The differences in these lower limits were due to different dilution factors we had to apply in order to eliminate inhibition of the qPCR reaction (see supporting information). Interestingly, in the case of Mais-down (Figure 1), Mais-up (Figure 2), Ditch (Figure 4b), and Bloop (Figure 5), the falling limbs of the NaCl BTCs were less steep than of T23, while in the case of Heuwelerbach (Figure 3) and Gloop (Figure 4a), the shapes of the BTCs of both NaCl and T23 were similar. Finally, for a number of BTCs, at the end of the experiment, we observed one or two samples with a "raised" concentration (e.g., Ditch at 58 min; Figure 4a).

3.3. Determining the NaCl and T23 Mass Balance: Estimates From Field Data

[30] The recovered T23 mass ranged from 2.9% for the Heuwelerbach to 52.6% for the Bloop (Table 3). The recovery of the NaCl tracer ranged between 66.7% (Mais up) and 106.1% (Bloop) (Table 4). The results in the Bloop showed nearly complete salt recovery and 46.4–52.6% T23 mass recovery. Finally, the Heuwelerbach showed the largest difference in recovery: 2.9–6.0% T23 versus 94.3–97.2% NaCl. From these results, we concluded that T23 mass recovery was always lower than mass recovery of NaCl. Also, there was no relationship between mass recoveries of T23 and NaCl.

3.4. Batch Experiments

[31] The field batch experiments with brook water (Figure 6) were carried out parallel to the T23 tracer injection experiment in a separate batch container for the entire duration of the experiment with the objective to study T23 decay or inactivation. The duration of the batch experiments was variable but all were rather short (<3.5 h), which was identical to the duration of the field experiments. For example, the duration of the Ditch field batch experiment was only 75 min, while the duration of the Bloop field batch experiment was more than 200 min. From Figure 6, we observed that the mass of T23 in the batch container did not change over time, so decay or inactivation for the duration of the injection experiment was not detected. In addition, we observed that there was a remarkable and statistically significant difference between the T23 mass injected and the mass measured in the batch container. Immediately from the start of the batch experiment, and within minutes after mixing the injected T23

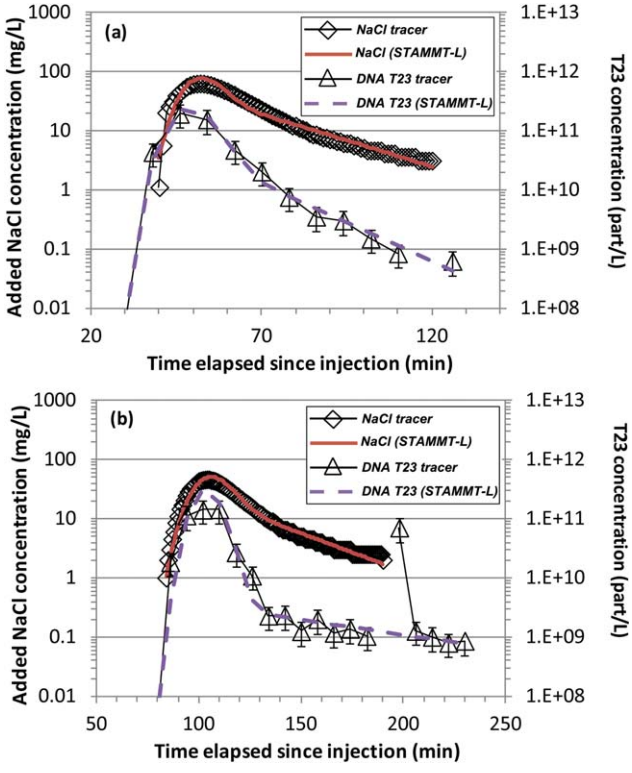

Figure 5. Bloop experiments. BTCs of salt and DNA tracer T23 (a) 300 m and (b) 550 m downstream of the point of tracer injection. Error bars indicate 95% confidence intervals.

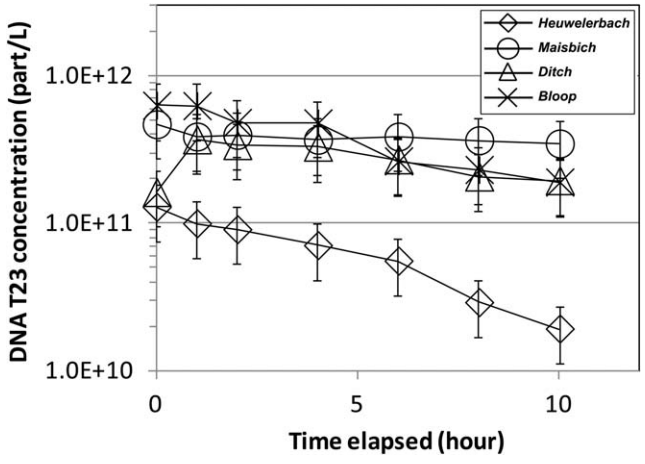

Figure 7. Batch experiments with brook water and sediment for T23. Error bars indicate 95% confidence intervals.

mass with brook water, the difference between injected mass and recovered mass was established and remained unchanged for the duration of the experiments. Furthermore, in the batches, the differences between injected mass and recovered mass were not the same for the various brooks: for Bloop, the average percentage of recovered mass was 18%, for the Heuwelerbach 11%, and for the Ditch the recovered DNA tracer mass was 3%. Although field batch experiments of only three brooks are shown in Figure 6, the Maisbich and Gloop had a similar pattern: no decay or inactivation, and the percentages of recovered over injected mass were 37 and 60%, respectively. We did not fully understand this brook dependent instantaneous loss. However, when T23 was injected into 100 mL MilliQ water, during the preliminary steps of the development of the protocol (see supporting information), no losses occurred.

[32] The batch experiments with brook water and sediment had a total duration of 10 h (Figure 7) and were aimed at determining the magnitude of T23 mass interaction with brook bottom sediment. Due to the rather coarse nature of most of the brook sediments, the sediment in the batch remained at the bottom of the batch container for the entire duration of the experiment, as was also observed in the field. From the figure, we observed that T23 concentrations for the Maisbich, Bloop, and Heuwelerbach slowly reduced

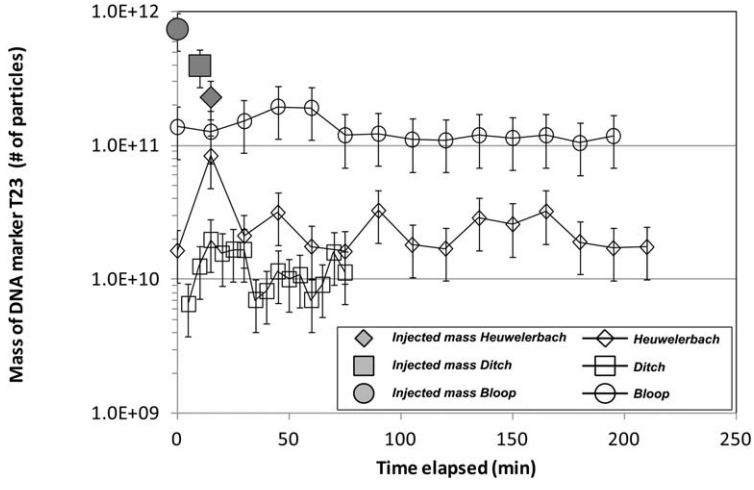

Figure 6. Field batch experiment with Heuwelerbach, Ditch, and Bloop water; DNA tracer T23 mass = total mass present in 100 ml batch with brook water. Please note that injection of T23 mass for all batch experiments was at time elapsed = 0 min, but were given a horizontal offset for clarity. Error bars indicate 95% confidence intervals.

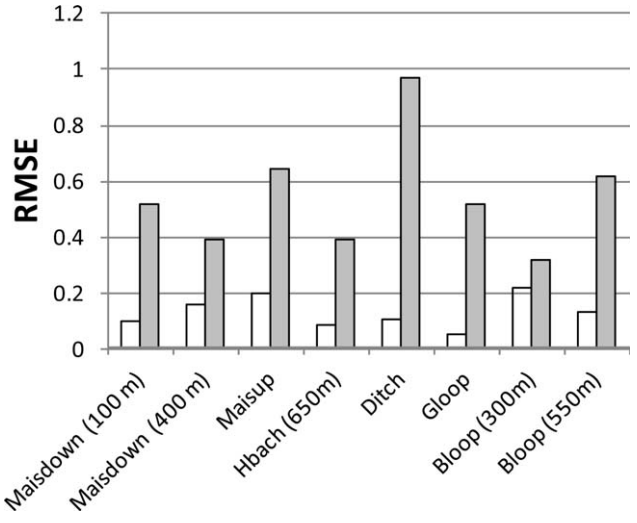

Figure 8. Normalized root of the mean squared values (RMSE) of the T23 (gray bars) and NaCl BTCs for each injection experiments, determined with STAMMT-L.

in a log linear fashion. Because of the absence of decay in the batches without sediment, we concluded that T23 mass slowly attached or sorbed to the sediment. Assuming a first-order process, we calculated attachment rate coefficients ranging from negligible for the Ditch to 0.03 hr^{-1} for the Maisbich, 0.12 hr^{-1} for the Bloop, and 0.19 hr^{-1} for the Heuwelerbach.

3.5. Comparing the Tracer Performance of NaCl and T23 with STAMMT-L

[33] Because STAMMT-L cannot model changing stream parameters in space (e.g., more than one reach of a stream), each measured BTC (e.g., Bloop at 300 m and at 550 m) was considered to be a stand-alone injection experiment. The fitted curves are given in Figures 1–5 as colored lines for NaCl (brown) and T23 (purple). For the evaluation of parameter values, we excluded the T23 BTC of the Heuwelerbach at 300 m, since the first part of the BTC was not sampled.

[34] The normalized root of the mean squared error (RMSE) [e.g., *Gooseff et al*., 2003] of all NaCl BTCs was between 0.1 and 0.2, which was 1–5 times lower than the RMSE of the T23 BTCs (Figure 8; values are given in Table 5). This was because of the lower number of data points of the T23 BTCs compared to the NaCl BTCs and because of the presence of false positives in some of the T23 BTCs. In general, fitted flow velocities and longitudinal dispersivities of NaCl and T23 transport were similar (Figures 9a and 9b). In one case (Gloop), the longitudinal dispersivity of the T23 BTC was much larger (2.74 m) than of the NaCl BTC (0.22 m). We attributed this to the relatively low mass of injected salt in combination with the high discharge (89 L/s), resulting in an underdeveloped, small, NaCl peak, which passed rapidly and without tailing. The coefficients of determination between fitted velocities of NaCl and T23 and fitted longitudinal dispersivities of NaCl and T23 (omitting Gloop) were 0.98 and 0.68, respectively, which we considered to be very good and good.

[35] The ratio of storage cross-sectional area to stream cross-sectional area, β_{tot}, was larger for NaCl than for T23. Since fitted flow velocities for NaCl and T23 were similar, larger β_{tot} values indicated that the fitted storage zone areas for NaCl were larger than for T23.

[36] We found that values of $\beta\omega$, the storage zone exchange coefficient, determined from the T23 BTCs ($(\beta\omega)_{T23}$), were half of the values determined from the NaCl BTCs ($(\beta\omega)_{NaCl}$) with $R^2 = 0.90$ (Figure 9c). The presence of storage zone areas and storage zone exchange coefficients for NaCl indicated that in all experiments there was exchange of NaCl between brook and storage zone(s), which was rapid and within the timeframe of the experiment. Mass dilution factors for NaCl in the range of 0.95–1.49 (Table 5) indicated that 0–32.8% NaCl mass did not pass the measuring points and was stored in the brook environment, either in surface storage zones, in the hyporheic zone or on its way to recharge groundwater. For T23, fitted storage zone areas were smaller, and so were storage zone

Table 5. Parameter Values (± One Standard Deviation) Determined From Fitting Measured BTCs with a Nonlinear Least Squares Algorithm in STAMMT-L

NaCl	v	β_{tot}	α	ω	φ
Maisdown (100 m)	0.16 ± 0.006	0.07 ± 0.077	0.49 ± 0.107	6.86E-3 ± 3.40E-4	1.02 ± 0.043
Maisdown (400 m)	0.44 ± 0.021	0.17 ± 0.168	0.30 ± 0.328	1.83E-2 ± 1.73E-3	1.26 ± 0.063
Maisup	0.12 ± 0.010	0.37 ± 0.061	0.46 ± 0.093	2.18E-3 ± 8.97E-5	1.49 ± 0.047
Hbach (650 m)	0.20 ± 0.026	0.11 ± 0.294	0.29 ± 0.384	1.86E-2 ± 2.73E-3	1.15 ± 0.083
Ditch	0.10 ± 0.003	0.10 ± 0.038	0.88 ± 0.029	1.68E-3 ± 9.53E-5	1.18 ± 0.020
Gloop	0.34 ± 0.016	0.17 ± 0.119	0.22 ± 0.240	2.38E-2 ± 1.92E-3	1.01 ± 0.026
Bloop (300 m)	0.10 ± 0.009	0.24 ± 0.055	1.69 ± 0.087	9.57E-4 ± 6.66E-5	0.95 ± 0.035
Bloop (550 m)	0.09 ± 0.003	0.13 ± 0.026	1.87 ± 0.032	6.46E-4 ± 1.97E-5	1.04 ± 0.018
DNA	V	β_{tot}	α	ω	φ
Maisdown (100 m)	0.17 ± 0.027	0.03 ± 0.554	0.25 ± 0.320	9.43E-3 ± 1.93E-3	2.96 ± 0.381
Maisdown (400 m)	0.41 ± 0.039	0.08 ± 0.599	0.39 ± 0.379	1.69E-2 ± 5.01E-3	6.26 ± 0.250
Maisup	0.13 ± 0.038	0.02 ± 1.256	0.60 ± 0.243	7.12E-3 ± 9.30E-3	18.07 ± 0.324
Hbach (650 m)	0.21 ± 0.039	0.08 ± 0.613	0.15 ± 0.761	1.58E-2 ± 7.02E-3	34.76 ± 0.255
Ditch	0.09 ± 0.026	0.05 ± 0.511	0.50 ± 0.195	1.70E-3 ± 8.22E-4	7.10 ± 0.401
Gloop	0.29 ± 0.024	0.01 ± 0.563	2.74 ± 0.135	3.85E-3 ± 1.76E-3	4.91 ± 0.235
Bloop (300 m)	0.10 ± 0.018	0.05 ± 0.257	2.14 ± 0.090	1.08E-3 ± 1.60E-4	1.97 ± 0.167
Bloop (550 m)	0.09 ± 0.010	0.04 ± 0.671	1.07 ± 0.102	2.01E-4 ± 1.07E-4	1.55 ± 0.302

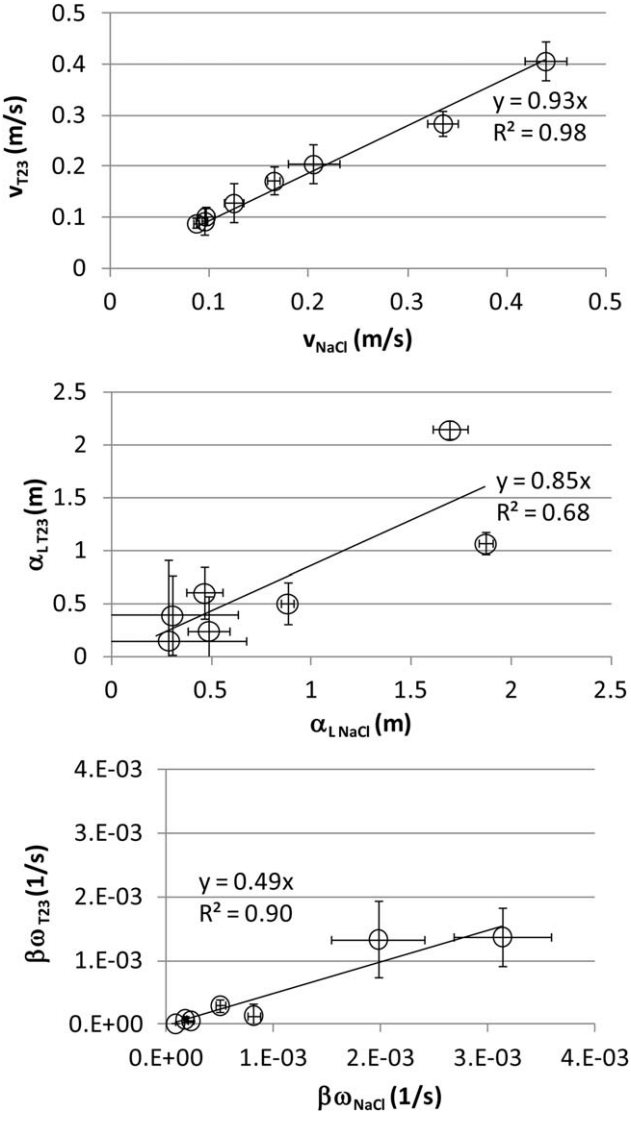

Figure 9. (top) Relation between fitted flow velocity, (middle) fitted longitudinal dispersivity, and (bottom) storage zone exchange coefficient of T23 and NaCl BTCs. All values were determined with STAMMT-L. Error bars indicate two standard deviations.

exchange coefficients, despite the fact that T23 had traveled the same distance in the brook, while T23 mass dilution factors ranged from 1.6 to 34.8.

4. Discussion

4.1. Hydrological Aspects of Synthetic DNA Tracing

[37] Compared to *Foppen et al*. [2011], in this current work, we improved the protocols for experimental design and laboratory analysis work. Also, the uniqueness of the artificial DNA sequence was screened more thoroughly by using more screening criteria. Furthermore, the use of a Taqman probe to assist in determining synthetic DNA tracer concentrations improved the accuracy of the methodology. Finally, we were able to quantify synthetic DNA confidence limits. As a result, the data presented in this work were much more consistent than those reported by *Foppen et al*. [2011]. The latter had highly irregular mass balance results between first and second measurement point (19–122%), while for several tracers, mass recovery at the second downstream measurement point was twice as much compared to the first measurement point after tracer injection. We found that, within a flow velocity range of 0.1–0.5 m/s and for discharge values <100 L/s, there was no relationship between total mass recoveries of T23 and of NaCl determined from field data; instead, those recoveries seemed more associated with tracer characteristics in a particular brook than with stream hydraulic processes. However, the lower recovery in Mais-up (66.7% NaCl (Table 4) and 6.8% T23 (Table 3)) could be influenced by the presence of a well-identified hyporheic exchange zone [*Westhoff et al*., 2011]. Despite this observed lack of relationship between T23 and NaCl total mass recovery, advective and dispersive transport of both NaCl and T23 were very similar. Furthermore, fitted storage zone areas and storage zone exchange coefficients of NaCl were larger than of T23, while the fitted mass dilution factor of T23 was larger than of NaCl. From the combination of these three differences between T23 and NaCl, we inferred that exchange of T23 with storage zones, which surely took place, was obscured by the disappearance of a part of the T23 mass. As a consequence, artificial DNA can be used mainly to determine advective and dispersive transport in the brook, but, at least at this stage, not to assess conservative solute mass exchange processes related to surface transient storage or hyporheic exchange. Coming back to our original objective, when comparing salt and synthetic DNA in the stream tracer injection experiments, we carried out, for determining solute exchange with transient storage zone(s), the performance of salt was superior to that of synthetic DNA.

[38] The T23 mass losses could be explained by attachment or sorption of T23 in the storage zone(s) and by immediate and instantaneous losses of T23 upon introduction into the brook, and in case of the Maisbich, Ditch, and Bloop, because of the low-attachment rate coefficient (Figure 7), most of the mass lost was more likely due to initial loss than due to attachment or sorption to sediment. We hypothesize that these initial losses were, on the one hand, a characteristic of the DNA tracer material, and, on the other hand, dependent on brook water quality. We ruled out sorption of T23 to suspended solids, which were of course present in the brook waters we used. Also, we ruled out instantaneous ingestion or digestion of T23 by microorganisms. If one of these processes would be a sink for T23 mass, then we would have expected these to be dependent on time, or to result in the complete loss of T23 mass upon injection into the brook, which obviously did not occur. We do not know the cause of the high initial losses of DNA tracer material. One reason could be that the quality of the produced DNA tracer is not constant, and the vial with DNA obtained from the producer contains a collection of DNA molecules of varying quality. Then, when injected into brook water, integrity of a part of the DNA is affected, either making it impossible for the Taq polymerase to amplify these compromised DNA tracer molecules, or causing disintegration of a fraction of the injected DNA mass, or a combination of both. Another reason could be the presence of small quantities of trivalent or multivalent positively charged ions, causing DNA molecules to

"jump" into a state of cation-induced "toroidal"-shaped condensation, whereby the DNA molecules can rapidly shrink to a fraction of their original size [*Andresen et al*., 2008; *Hackl et al*., 2005; *Kasyanenko et al*., 2010; *Widom and Baldwin*,1980]. In this respect, the presence of relatively high trivalent Al-concentrations in the Ditch water (see supporting information Table S1) could have contributed to the high initial losses of DNA tracer observed in the Ditch experiments. However, this does not allow us to explain the large initial loss in the Heuwelerbach experiments. It is clear that the aspect of initial losses requires attention in future research on this topic in order to arrive at a robust use of synthetic DNA as tracer in hydrological applications.

[39] Another aspect that deserves attention is the seemingly random occurrence of raised T23 concentrations (sudden spikes in the measured BTCs), which were in part responsible for the higher RMSE values of the T23 BTCs than the ones of the NaCl BTCs. We attribute this to the brook water quality. In each sample that was prepared for qPCR analysis, there was a small quantity of brook water present of which the quality could not be controlled. The PCR reaction is driven by the enzyme Taq polymerase, and its activity is directly dependent on water quality. It seemed likely that in some of the samples compounds were present, which may have increased the Taq polymerase activity, thereby giving rise to a kind of false positive effect on measured DNA concentrations. The number of false positives was not high, but this unwanted and confounding effect requires attention in future research.

4.2. Environmental Considerations of Synthetic DNA Tracing

[40] At this point, and before discussing potential future research and applications of synthetic DNA, discussing the safety aspects of introducing DNA tracers in the environment is merited. Although DNA is natural, and can be considered to be a small piece of "organic matter," the use of synthetic or custom made DNA in the environment might raise questions. No evidence exists that DNA is toxic to any flora or fauna [*Nielsen et al*., 2007; *Lorenz and Wackernagel*, 1994]. In fact, phosphorus in extracellular DNA, present in aqueous environments, is usually considered a food source for many organisms [e.g., *Dell'Anno and Danovaro*, 2005; *Siuda et al*., 1998]. As was stated before, the synthetic DNA tracer we used was single stranded (usually, DNA is double stranded). Because of this characteristic, the likelihood for transformation to occur is low [*Nielsen et al*., 2007; *Lorenz and Wackernagel*, 1994]. Transformation is the process whereby extracellular DNA is taken up in the genetic material of naturally occurring bacteria. Extensive literature has demonstrated that transformation occurs at a large scale in nature, but only with double-stranded DNA. Single-stranded DNA material seems an inefficient substrate for transformation, and therefore we believe that the risk of creating genetically modified organisms (GMOs) is low or even absent. Furthermore, the DNA tracers we used were not "open reading frames" (ORF). An ORF is a certain sequence of nucleotides, which signals enzymes, involved in the replication of DNA for mRNA production, where to start and to stop transcribing DNA. With ORFs, and if incorporated in the genomic material of bacteria, mRNA can be produced, which is responsible for the production of amino acids and, finally, for the production of proteins, which can be potentially harmful.

4.3. Future Applications

[41] As we indicated earlier, with synthetic DNA a theoretically unlimited number of different tracers can be designed, which can be used to assess different flow paths and travel times at the same time in catchments and in fractured aquifers. The latter was already demonstrated by Sabir and workers [*Sabir et al*., 1999, 2000]. Using synthetic DNA in "single-tracer mode," determining longitudinal dispersion and travel times in rivers might be an important future area of application for DNA tracers, for instance in relation to river water intake points for water supply. This type of application, which does not require the determination of all components of the mass balance, could also be extremely useful in "multi-tracer mode" for medium to large-scale source area applications in complex areas, like karstic limestone areas. The use of small DNA fragments (SDFs) [e.g., *Sargent et al*., 2011; *Luchetti et al*., 2012] make it possible to purchase small, tailored, DNA fragments, and use these as DNA tracer, in quantities up to 10^{19} particles, which is 1000 times more than what we applied, for USD 1000–5000. To illustrate the potential of synthetic DNA in those cases, we implemented the analytical solution of the 1-D transient transport equation with a term for first-order decay, μ [e.g., *Bear*, 1972; *Van Genuchten and Alves*, 1982] in a spreadsheet. The dispersion coefficient was estimated using a set of polynomials developed by *Deng et al*. [2002]. For a design river with a width of 75 m, a depth of 1.5 m, a discharge between 10 and 50 m^3/s, and assuming a DNA decay rate coefficient ranging between 0.1 and 0.5 day^{-1}, the maximum distance between point of injection of synthetic DNA and point of measurement could be as much as 275 km, which we consider to be a very large distance for tracer injection experiments.

[42] Furthermore, we anticipate that when causes of initial DNA tracer losses are known and can be quantified, in small-scale applications the combined use of reactive DNA tracers and conservative tracers, augmented with carefully designed batch experiments to determine decay rate coefficients and sorption rate coefficients, will yield a better understanding of storage processes occurring in the brook and of interactions of the brook with its environment.

[43] Finally, synthetic DNA is a reactive tracer and a small piece of organic material, which decays and interacts with compounds in surface water and possibly also in groundwater. Recognizing that DNA is a common constituent of particulate organic matter and one of the most important phosphorus sources for microplankton in aquatic environments [*Siuda et al*., 1998], we hypothesize that synthetic DNA could be a marker used to better assess the transport and fate of organic matter in aquatic systems and to elucidate phosphorus-related processes in complex food chains involving extracellular DNA and organic phosphorus.

5. Conclusions

[44] We carried out six stream tracer injection experiments with both NaCl and synthetic DNA tracer (T23) in various streams in Netherlands, Belgium, and Luxembourg.

[45] 1. In contrast to the work of *Foppen et al*. [2011], in the present work, we increased the reliability and accuracy of the entire DNA tracer injection method by the stepwise identification and application of revised and improved protocols for sample taking, sample storage, and DNA tracer analysis. In addition, we used a Taqman probe with a length of 25 nucleotides to detect synthetic DNA concentrations during qPCR analysis. This further increased the accuracy of the method. As a result of the implementation of these improvements in the DNA stream tracer injection methodology, we concluded that:

[46] a. Within a flow velocity range of 0.1–0.5 m/s and for discharge values $<$100 L/s, advective and dispersive transport of both NaCl and T23 fitted with STAMMT-L were very similar.

[47] b. Fitted storage zone areas and storage zone exchange coefficients of NaCl were larger than of T23, while the mass dilution factor of T23 was larger than of NaCl. Together, these comparative findings made clear that exchange of T23 with storage zones was obscured by the disappearance of a part of the T23 mass.

[48] c. The Root of the Mean Squared Error of the differences between measured and with STAMMT-L fitted data of NaCl BTCs was 1–5 times lower than of T23 BTCs.

[49] d. Based on batch experiments, we inferred that the disappearance of a part of the T23 mass in most stream tracer injection experiments was mainly caused by initial T23 losses. Irreversible sorption or attachment to bed sediment also played a role, while decay was not important.

[50] e. For brooks with a flow velocity $<$0.5 m/s and a discharge $<$100 L/s, artificial DNA could be used to determine advective and dispersive transport in the brook, but not to assess solute mass exchange processes related to surface transient storage or hyporheic exchange. In this respect, the use of salt was superior to the use of artificial DNA.

[51] 2. To implement the method, a well-equipped microbiological laboratory is required, and this is usually not available in typical water research institutes. However, we believe that the qPCR technique is well-established, and therefore, collaborations with microbiological laboratories are the obvious way forward.

[52] 3. Future research on the DNA tracer methodology has to focus on causes and quantification of initial DNA tracer losses and on reducing the occurrence of false positives in determining DNA tracer concentrations. Also, the long-term behavior of synthetic DNA tracer needs to be explored.

[53] **Acknowledgments.** The authors want to express their gratitude to the Centre Recherche Public Gabriel Lippmann in Luxembourg for their support. T.B. wants to thank all colleagues at CRP Gabriel Lippmann for their time and scientific discussion on tracer hydrology during his research visits in 2011 and 2012. This research is financially supported by the Netherlands Fellowship Program and by a Mobility-of-Researchers grant of the FNR Luxembourg. J.W.F. wants to thank Roy Haggerty for his useful and constructive comments on the results obtained with STAMMT-L. The authors want to acknowledge the constructive reviews of Ricardo González-Pinzón, two anonymous reviewers and the editor, Selker, which improved the quality of the data analysis and the focus of the paper.

References

Aleström, P. (1995), Novel method for chemical labelling of objects, Int. Pat. Appl. PCT/IB95/01144 and Publ. WO 96/17954, World Intel. Prop. Organ. [Available at http://www.wipo.int/portal/index.html.en.]

Andresen, K., X. Qiu, S. A. Pabit, J. S. Lamb, H. Y. Park, L. W. Kwok, and L. Pollack (2008), Mono- and trivalent ions around DNA: A small-angle scattering study of competition and interactions, *Biophys. J.*, *95*, 287–295.

Bear, J. (1972), *Dynamics of Fluids in Porous Media*, Elsevier, New York.

Briggs, M. A., M. N. Gooseff, C. D. Arp, and M. A. Baker (2009), A method for estimating surface transient storage parameters for streams with concurrent hyporheic storage, *Water Resour. Res.*, *45*, W00D27, doi:10.1029/2008WR006959.

Bustin, S. A., and T. Nolan (2009), Analysis of mRNA expression by real time PCR, in *Real-Time PCR. Current Technology and Applications*, edited by J. Logan, K. Edwards, and N. Saunders, Caiser Academics, Norfolk, U. K.

Choi, J., and J. W. Harvey (2000), Characterizing multiple timescales of stream and storage zone interaction that affect solute fate and transport in streams, *Water Resour. Res.*, *36*(6), 1511–1518.

Darling, W. G., D. C. Gooddy, J. Riches, and I. Wallis (2010), Using environmental tracers to assess the extent of river-groundwater interaction in a quarried area of the English Chalk, *Appl. Geochem.*, *25*, 923–932.

Dell'Anno, A., and R. Danovaro (2005), Extracellular DNA plays a key role in deep-sea ecosystem functioning, *Science*, *309*(5744), 2179.

Deng, Z. Q., L. Bengtsson, V. P. Singh, and D. D. Adrian (2002), Longitudinal dispersion coefficient in single-channel streams, *J. Hydraul. Eng.*, *128*(10), 901–916, doi:10.1061/(ASCE)0733-9429(2002)128:10(901).

Foppen, J. W., C. Orup, R. Adell, V. Poulalion, and S. Uhlenbrook (2011), Using multiple artificial DNA tracers in hydrology, *Hydrol. Processes*, *25*, 3101–3106.

Gaillard, C., and F. Strauss (2000), Eliminating DNA loss and denaturation during storage in plastic microtubes, *Am. Biotechnol. Lab.*, *18*(13), 24.

Gerrits, A. M. J. (2010), The role of interception in the hydrological cycle, PhD thesis, Delft Univ. of Technol., Delft, Netherlands. [Available at http://repository.tudelft.nl].

Gooddy, D. C., W. G. Darling, C. Abesser, and D. J. Lapworth (2006), Using chlorofluorocarbons (CFCs) and sulphur hexafluoride (SF6) to characterise groundwater movement and residence time in a lowland Chalk catchment, *J. Hydrol.*, *330*, 44–52.

Gooseff, M. N., et al. (2003), Comparing transient storage modeling and residence time distribution (RTD) analysis in geomorphically varied reaches in the Lookout Creek basin, Oregon, USA, *Adv. Water Resour.*, *26*(9), 925–937, doi:10.1016/S0309-1708(03)00105-2.

Gooseff, M. N., D. A. Benson, M. A. Briggs, M. Weaver, W. Wollheim, B. Peterson, and C. S. Hopkinson (2011), Residence time distributions in surface transient storage zones in streams: Estimation via signal deconvolution, *Water Resour. Res.*, *47*, W05509, doi:10.1029/2010WR009959.

Gourcy, L., and A. Brenot (2011), Multiple environmental tracers for a better understanding of water flux in a wetland area (La Bassée, France), *Appl. Geochem.*, *26*, 2147–2158.

Hackl, E. V., S. V. Kornilova, and Y. P. Blagoi (2005), DNA structural transitions induced by divalent metal ions in aqueous solutions, *Int. J. Biol. Macromol.*, *35*, 175–191.

Haggerty, R., and P. Reeves (2002), STAMMT-L Version 1.0 User's Manual, Rep. ERMS 520308, 76 pp., Sandia Natl. Lab., Albuquerque, N. M.

Haggerty, R., E. Martí, A. Argerich, D. von Schiller, and N. B. Grimm (2009), Resazurin as a "smart" tracer for quantifying metabolically active transient storage in stream ecosystems, *J. Geophys. Res.*, *114*, G03014, doi:10.1029/2008JG000942.

Harvey, J. W., B. J. Wagner, and K. E. Bencala (1996), Evaluating the reliability of the stream tracer approach to characterize stream-subsurface water exchange, *Water Resour. Res.*, *32*(8), 2441–2451, doi:10.1029/96WR01268.

Juilleret J., J. F. Iffly, L. Hoffmann, and C. Hissler (2012), The potential of soil survey as a tool for surface geological mapping: A case study in a hydrological experimental catchment (Huewelerbach, Grand-Duchy of Luxembourg), *Geol. Belg.*,*15*, 36–41.

Kasyanenko, N. A., D. A. Mukhin, and I. Y. Perevyazko (2010), Conformational changes of a DNA molecule induced by metal complexes formed in solution, *Polym. Sci. Ser. C*, *52*(1), 122–133.

Lamontagne, S., F. W. Leaney, and A. L. Herczeg (2005), Groundwater-surface water interactions in a large semi-arid floodplain: Implications for salinity management, *Hydrol. Processes*, *19*, 3063–3080.

Leibundgut C., P. Malozewski, and C. Külls (2009), *Tracers in Hydrology*, John Wiley, Chichester, U. K.

Lorenz, M. G., and W. Wackernagel (1994), Bacterial gene transfer by natural genetic transformation in the environment, *Microbiol. Rev. 58*, 563–602.

Luchetti, A., A. Filareto, M. Sanchez, G. Ferraguti, M. Lucarelli, et al. (2012), Small fragment homologous replacement: Evaluation of factors influencing modification efficiency in an eukaryotic assay system, *PLoS One*, *7*(2), e30851, doi:10.1371/journal.pone.0030851.

Négrel, P., and H. Pauwels (2004), Interaction between different groundwaters in Brittany catchments (France): Characterizing multiple sources through strontium- and sulphur isotope tracing, *Water Air Soil Pollut.*, *151*, 261–285.

Négrel, P., and E. Petelet-Giraud (2005), Strontium isotopes as tracers of groundwater induced floods: The Somme case study (France), *J. Hydrol.*, *305*, 99–119.

Nielsen, K. M., P. J. Johnsen, D. Bensasson, and D. Daffonchio (2007), Release and persistence of extracellular DNA in the environment—Review, *Environ. Biosafety Res.*, *6*, 37–53, doi:10.1051/ebr:2007031.

Oxtobee, J. P. A., and K. Novakowski (2002), A field investigation of groundwater/surface water interaction in a fractured bedrock environment, *J. Hydrol.*, *269*, 169–193.

Runkel, R. L. (1998), One-dimensional transport with inflow and storage (OTIS): A solute transport model for streams and rivers, US Geol. Surv. Water Resour. Invest. Rep. 98–4018, 73 p.

Sabir, I. H., J. Torgersen, S. Haldorsen, and P. Aleström (1999), DNA tracers with information capacity and high detection sensitivity tested in groundwater studies, *Hydrogeol. J.*, *7*, 264–272.

Sabir, I. H., S. Haldorsen, J. Torgersen, P. Aleström, S. Gaut, H. Colleuille, T. S. Pedersen, and N.-O. Kitterød (2000), Synthetic DNA tracers: Examples of their application in water related studies, in *Tracers and Modelling in Hydrogeology* (Proceedings of the TraM 2000 Conference held at Liège, Belgium, May 2000), pp. 159–165, IAHS Publ. 262.

Sargent, R. G., S. Kim, and D. C. Gruenert (2011), Oligo/Polynucleotide-based gene modification: Strategies and therapeutic potential, *Oligonucleotides*, *21*(2), 55–75, doi:10.1089/oli.2010.0273.

Siuda, W., R. J. Chróst, and H. Güde (1998), Distribution and origin of dissolved DNA in lakes of different trophic states, *Aquat. Microb. Ecol.*, *15*(1), 89–96.

Van Genuchten, M. Th., and W. J. Alves (1982), Analytical solutions of the one-dimensional convective-dispersive solute transport equation, *U.S. Dep. Agric. Tech. Bull. 1661*, *151 p*.

Vengosh, A., J. Gill, M. L. Davisson, and G. B. Huddon (2002), A multiisotope (B, Sr, O, H, and C) and age dating (H-3-He-3 and C-14) study of groundwater from Salinas Valley, California: Hydrochemistry, dynamics, and contamination processes, *Water Resour. Res.*, *38*(1), 1008, doi:10.1029/2001WR000517.

Wagner, B. J., and J. W. Harvey (1997), Experimental design for estimating parameters of rate-limited mass transfer: Analysis of stream tracer studies, *Water Resour. Res.*, *33*(7), 1731–1741.

Ward, A. S., M. N. Gooseff, and K. Singha (2010), Imaging hyporheic zone solute transport using electrical resistivity, *Hydrol. Processes*, *24*(7), 948–953.

Westhoff, M. C., M. N. Gooseff, T. A. Bogaard, and H. H. G. Savenije (2011), Quantifying hyporheic exchange at high spatial resolution using natural temperature variations along a first-order stream, *Water Resour. Res.*, *47*, W10508, doi:10.1029/2010WR009767.

Widom, J., and R. L. Baldwin (1980), Cation-induced toroidal condensation of DNA studies with Co3+(NH3)6, *J. Mol. Biol.*, *144*, 431–453.

Zhao, S., and R. D. Fernald (2005), Comprehensive algorithm for quantitative real-time polymerase chain reaction, *J. Comput. Biol.*, *12*(8), 1047–1064.